Iranian Journal of Geophysics, Vol 20 No 6, 2027, Page 1 – 16 (Research Article)
DOI: 10.30499/ijg.2024.476972.1631

Investigation of anisotropy before and after Sisakht february 17, 2021 earthquake (Mn 5.4) using two independent methods: shear wave splitting and ambient noise interferometry

Mohadeseh Mohamadzadeh[1] Ahmad sadidkhouy [2*] and Ramin Movagharii[3]

[1] *M.Sc., Institute of Geophysics, University of Tehran, Tehran, Iran*
[2] *Associate Professor, Institute of Geophysics, University of Tehran, Tehran, Iran*
[3] *Postdoctoral research fellow, Southern University of Science and Technology, Shenzhen, Guangdong, China*

(Received: 07 December 2024, Accepted: 26 November 2024)

Abstract

This study investigates the anisotropic characteristics of seismic waves following the Sisakht earthquake on February 17, 2021, in the southwest of Iran. Our analysis of the anisotropic behavior of the region was conducted using two methodologies, shear wave splitting analysis (SWS) and ambient noise interferometry (ANI). These methods provided complementary insights into the subsurface dynamics influenced by seismic activity. The analysis of shear wave splitting used continuous seismic data from the Kolanja station, which included 237 aftershocks (earthquake that occurs after a larger seismic event) and 63 foreshocks (earthquake that occurs before a larger seismic event). This extensive dataset allows us to analyze seismic wave behavior before and after the earthquake. According to calculations, there was a significant shift in the orientation of fast-polarized S waves, which shifted from 114.5° prior to the earthquake to 93.46° following the earthquake. According to this shift, there may have been an alteration in subsurface material properties. This indicates that the earthquake may have impacted the alignment or stress distribution within the crust of the Earth. In addition, we have observed an increase in the time delay between the slow and fast-polarized S waves before and after the earthquake, with the delay increasing from 0.08±0.01 seconds before to 0.1±0.01 seconds after the earthquake. This change highlights modifications in wave propagation characteristics and suggests potential reconfiguration of subsurface structures due to seismic activity. There has been an apparent change in the direction of anisotropy as well, from NW-SE before the earthquake to NE-SW afterward, indicating that the stress fields or material alignments within the crust have been altered. In addition to shear wave splitting, we analyzed ambient noise data from ten seismological stations in the region. By retrieving empirical Green's functions (EGFs) between various station pairs, Anisotropic parameters were derived based on azimuthal variations of Rayleigh wave group velocities. According to the results, our findings of shear wave splitting were corroborated, with an overall anisotropy direction change of approximately 6 degrees across the study area correlating with previous findings. The consistency between the NW-SE direction of anisotropy identified through ambient noise interferometry and shear wave splitting results reinforces the reliability of these results. This study enhances our understanding of how seismic events influence anisotropic properties in the Earth's crust, contributing valuable insights into subsurface dynamics in seismically active regions.

Keywords: Seismic anisotropy, shear wave splitting, ambient noise interferometry, sisakht earthquake

[*]Corresponding author: asadid@ut.ac.ir

1 Introduction

The Iranian plateau, situated at the convergence between the Arabian and Eurasian plates, is characterized by complex tectonic activity that has shaped its present-day topography and seismicity. These characteristics made it a natural laboratory to investigate strong deformation in continental collision zones. The Zagros region resulting from this collision on the Arabian lithosphere, represents one of the most prominent and well-studied fold-and-thrust belts (e.g., Hatzfeld & Molnar, 2010; Mahmoodabadi et al., 2020; Motaghi et al., 2017; Movaghari & Doloei, 2020; Paul et al., 2010; Zarunizadeh et al., 2024, among others) in the world. Different parts of the Zagros belt, including the NW Zagros, the central Zagros, and the SE Zagros, exhibit distinct geological, structural, and tectonic characteristics, reflecting the varying nature of the forces acting upon them (e.g., Mouthereau et al., 2012).

The study of seismic anisotropy has provided valuable information over the past few decades for interpreting and evaluating active crustal deformation and stress fields using multiple anisotropic interpretation models (Becker et al., 2008; Boness & Zoback, 2006). Anisotropy in the Earth's crust may be caused by fluid-filled fractures or microcracks, by layered bedding in sedimentary formations, or by highly foliated metamorphic rocks (Crampin & Peacock, 2008). Anisotropy resulting from aligned cracks in the crust can be used to assess the state of stress in the crust (Pastori et al., 2012).

There are some radial and azimuthal seismic anisotropy studies on a regional scale beneath the Iran plateau (e.g., Kaviani et al., 2021; Movaghari et al., 2021; Sadeghi‐Bagherabadi et al., 2018). Previous studies show that anisotropy in a region is associated with significant changes before an earthquake (Chao & Peng, 2009). The development of methods for measuring anisotropy goes back to the last few decades (Crampin, 1985). Today, it has been proven that shear wave splitting (SWS) is one of the inevitable characteristics of any anisotropic medium. Because one of the reasons for anisotropy is the accumulation of stress in the rock mass. As a result of this stress accumulation, a shear wave entering an anisotropic region is split into two shear waves polarized at right angles according to the local symmetry of the medium (Crampin, 1985). The polarization direction of the fastest wave is known as the fast direction (ϕ), while the lag of the slower wave is known as the delay time (δt).When they exit the anisotropic medium, the fast shear wave maintains its polarization within the symmetry plane of that medium. Meanwhile, the time difference between the fast and slow shear waves serves as an indicator of the medium's anisotropy. In a fractured HTI medium, the polarization of the fast shear wave can help determine the orientation of the fractures, while the time delay between the fast and slow shear waves correlates with the intensity or density of the fractures (Vecsey et al., 2008).

Due to the complexity of the seismic shear-wave signal, it is difficult to measure seismic shear-wave splitting accurately. Various techniques have been developed to measure the time delays and polarizations of the fastest shear waves above small earthquakes (Crampin & Gao, 2006). There are two most commonly used techniques for estimating seismic anisotropy. The first is based on the covariance matrix decomposition,

and the second is based on the cross-correlation technique. The first one works better when the S-wave arrival is impulsive, which can be the case in very shallow volcanic earthquakes. Meanwhile, the second method works well when the slow component of the S-wave is visible and not quickly contaminated by later arrivals (Piccinini et al., 2013). In the cross-correlation method, it is assumed that, when a shear wave propagates in an anisotropic medium, it is split into orthogonally polarized fast and slow components that have an identical pulse shape. Therefore, the method seeks to maximize the cross-correlation between the corrected horizontal components, which corresponds mathematically to maximizing the determinant of the time-domain covariance matrix. Furthermore, if the shear wave is not separated and the particle motion is linear, the measurement will be null (Long & Silver, 2009).

In the last decade, another new method known as seismic interferometry has created a revolution in passive seismology. Developing seismic interferometric theory allows seismologists to extract useful information from the ambient noise wave, which is normally removed from seismic data. In this method, it is possible to extract short-period surface waves (Rayleigh and Love) from passive seismic data (Roux et al., 2005; Shapiro & Campillo, 2004). In a similar manner to shear waves, surface waves are sensitive to the anisotropic properties of the propagating medium and can be used to determine the properties of the earth's subsurface. This method uses cross-correlations of long time series of ambient noise recorded at two seismic stations (seismometers) to estimate Green's function between the two stations. The Green's function between two points may be interpreted as a seismogram recorded at one location in response to an impulsive or instantaneous source of energy at the other (Nicolson et al., 2012). The directional dependence of surface wave velocity extracted from ambient seismic noise can be used to determine azimuthal anisotropy (Forsyth, 1975; Smith & Dahlen, 1973).

The aim of this study is to investigate the variation of anisotropy of the Sisakht's February 20, 2021 earthquake in the southwest of Iran (Figure 1). At first shear wave splitting before and after the main event are studied, and the anisotropy parameters are calculated over a period of time. While shear wave splitting is an unambiguous indicator of anisotropy, the fact that it is typically a near-vertical path-integrated measurement means that splitting measurements generally lack depth resolution (Long & Silver, 2009). While it can detect time-dependent changes in anisotropy, SWS requires a dense distribution of seismic events to track these variations reliably. In areas with fewer earthquakes, this may result in data gaps that limit temporal resolution. In order to address these issues, ambient noise interferometry (ANI) method are used. Because different frequencies are sensitive to properties at different depths, surface wave dispersion can provide information about seismic velocity as it varies with depth (Nicolson et al., 2012). Using this method, we could determine the azimuthal anisotropy of the region in crustal depths. Azimuthal anisotropy describes the velocity variability regarding the propagation direction, which complements SWS measurements.

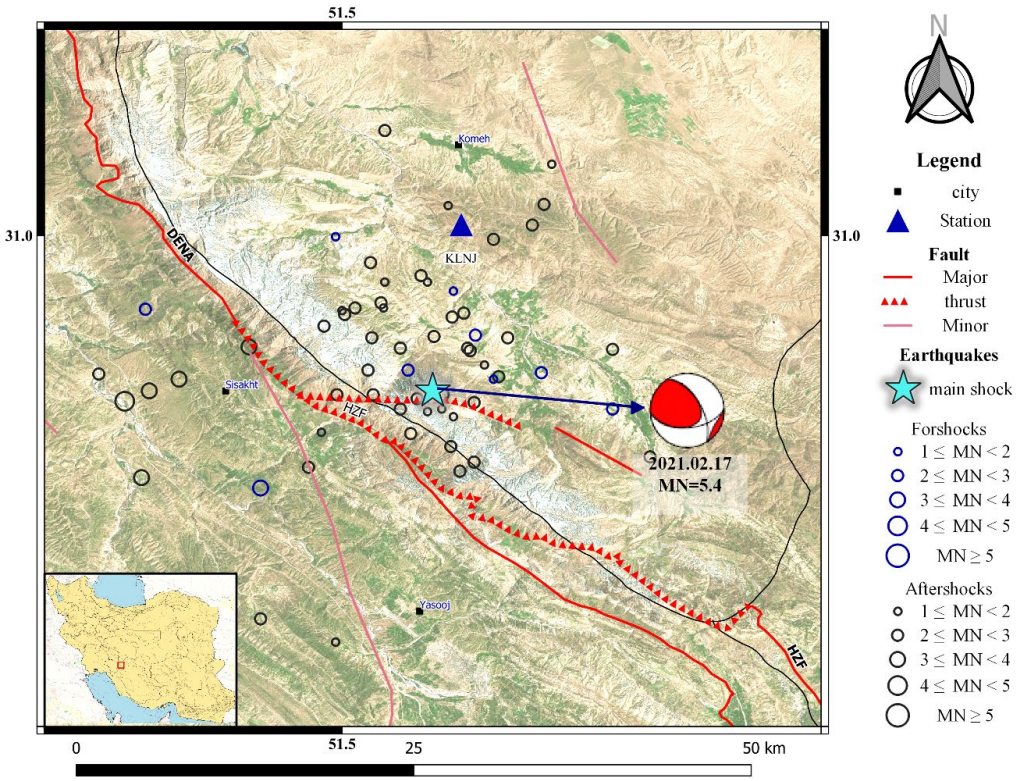

Figure 1. The epicenter and focal mechanism of the Sisakht February 17, 2021 earthquake and its foreshocks and aftershocks.

2 Seismotectonic and Seismicity

The Sisakht region is located in the Kohgiluyeh and Boyer-Ahmad Province, within the seismic province of Zagros and the Dena Mountain Range. This province encompasses both the Folded Zagros and the High Zagros regions, making it one of the most seismically active areas in Iran, characterized by the largest concentration of earthquake epicenters. Reverse strike-slip earthquakes and shear compression earthquakes are the most common types of seismic activity in this region, with focal depths ranging from 33 to 150 km. These earthquakes have a short return period and are generally of medium magnitude (Mirzaei et al., 1998). This region contains a part of Zagros and Sanandaj-Sirjan Zone (SSZ) and is located where the Main Zagros Reverse Fault (MZRF) and the Main Recent Fault (MRF) meet which can be considered as the border between NW Zagros and central Zagros. Figure 1 indicates that the Dena Fault, with its north-northwest trend and east-northeast dip, together with the High Zagros Fault, constitute a significant thrust fault system in the Zagros Mountains, which are near the epicenter of recorded seismic activity.

Statistical data indicate that relatively significant earthquakes have occurred in this region. According to Mousavi et al. (2014), 16 historical earthquakes with a magnitude (Mw) greater than 5 have been recorded. Additionally, during the first instrumental period (1900 to 1963), 15 earthquakes with a magnitude (Mw) exceeding 5 were documented. Figure 2 distribution of seismic events recorded in the Sisakht region.

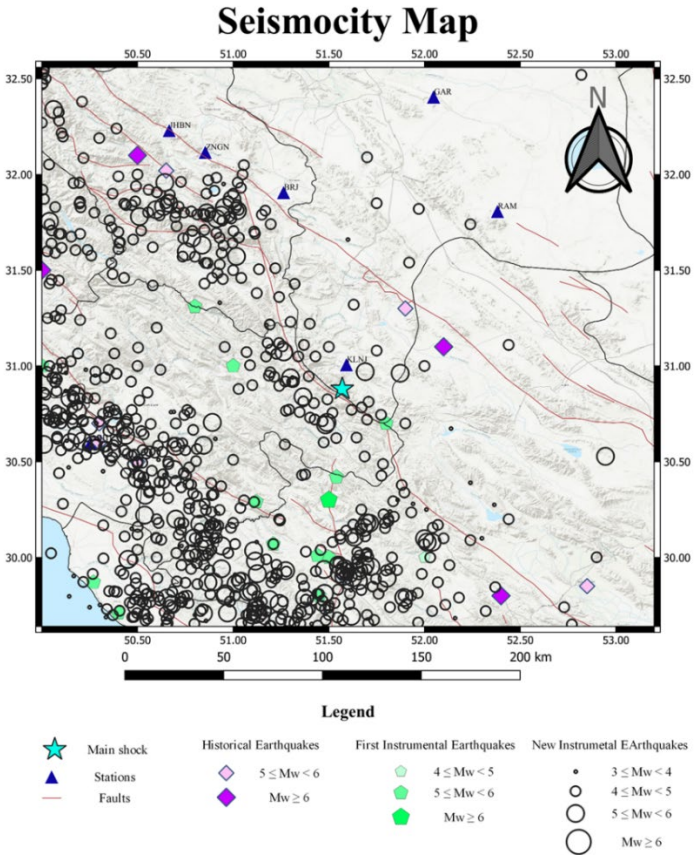

Figure 2. Seismicity of the region of this study.

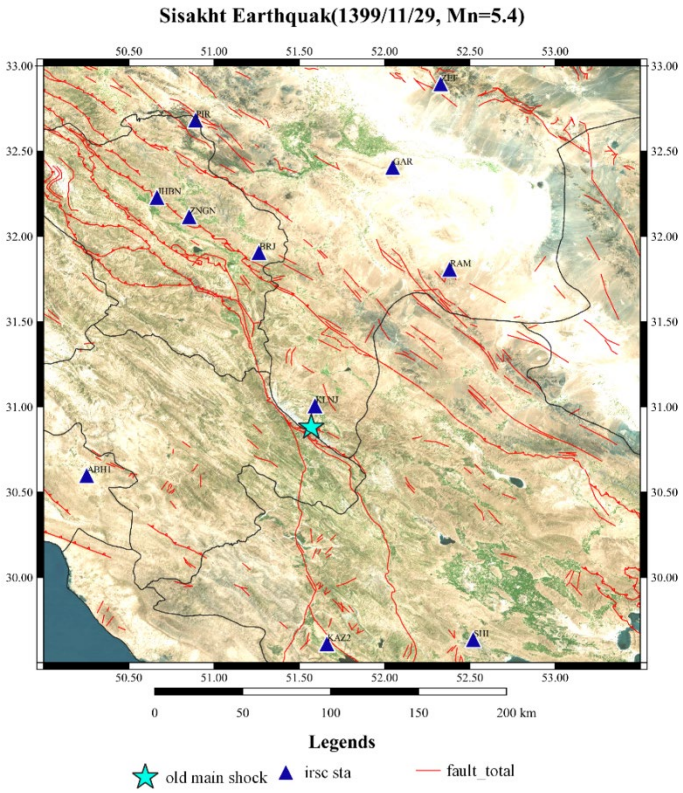

Figure 3. The seismological station's locations in this study area from the Iran seismological center (IRSC).

3 Data and Methodology

In this study, continuous seismic data were collected from ten seismographic stations Between the latitudes of 50° and 53.20° and the longitudes of 29.50° and 32.70° belonging to the Iranian Seismological Center (IRSC) for a period of one year prior to the earthquake until November 07, 2021. The locations of the stations used in this study are shown in Figure 3.

In the first step, the data availability of each station of our dataset were checked. Figure 4, shows the data availability by blue vertical lines which represent the number of one-hour signals per day during before and after the earthquake (red line in Figure 4). As we can see, two stations of KAZ2 and ABH1 have a huge gap after the earthquake. Therefore, due to irregular and the insufficient data during the entire study period, two stations of KAZ2 and ABH1, were excluded from the processing steps for ambient seismic noise analysis.

4.1 Shear Wave Splitting (SWS)

To study the anisotropy parameters (δt) and (ϕ), the data must be within the shear wave window, which means that the geometrical incidence angle must be between 0 and 45 degrees (Piccinini et al., 2013). In this regard, continuous data from the Kolanja (KLNJ) station, located 13.40 km from the main event were analysed. The data covered six months before and six months after the earthquake. We extracted 450 events that met the mentioned specifications for this study, we used a cross-correlation method implemented by the automatic code Anisomat+ to calculate the anisotropy parameters. Anisomat+ has been created and enhanced to swiftly extract crustal anisotropic parameters, specifically the fast polarization direction (ϕ) and delay time (dt), associated with shear wave splitting in seismic S-waves. This code consists of a collection of MATLAB scripts and functions that can assess these anisotropic parameters from three-component seismic recordings of local earthquakes using the cross-correlation method (Piccinini et al., 2013). Since there is no strong presence of topography gradients or fine structure scatters in the study of

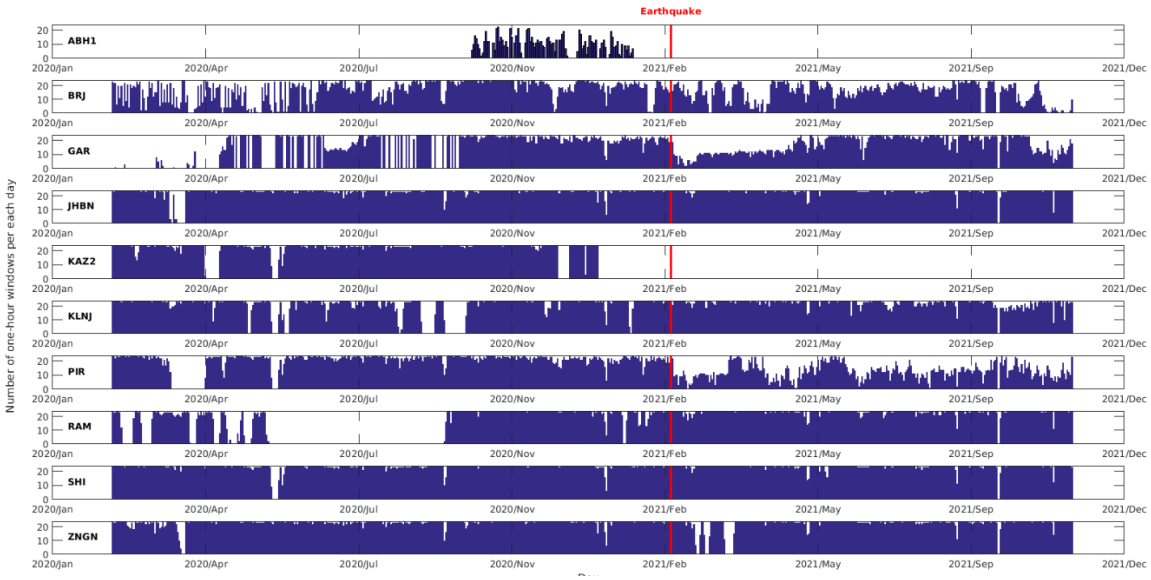

Figure 4. The seismological station's data availability. The vertical blue lines represent the number of one-hour signals per day, and the red lines show the day in which Sisakht's earthquake occurred.

seismic anisotropy in this tectonic region, and they are certainly less significant than in volcanic environments. Therefore, the cross-correlation method is a good choice for this study (Pastori et al., 2012).

The waveform cross-correlation method is applied to the horizontal components of the seismogram to measure the similarity of pulse shape between two S waves. These two waves have similar shapes and mutually orthogonal oscillation directions, and they travel with different velocities. The analysis involves selecting a frequency range that highlights the S waves and a time window for the analysis of the seismograms centered on the S arrival (the time window must include at least one S cycle) (Pastori et al., 2012).

A brief summary of the steps involved in this study is as follows: 1) detecting and cutting foreshocks and aftershocks from the continuous data of the KLNJ station, 2) editing the header and picking the arrival time of S and P phases, as well as converting to SAC, 3) calculating anisotropy parameters using the Anisomat+ code, 4) determining whether anisotropy parameters have changed before and after an earthquake.

The first three step was done using Obspy package in Python. ObsPy is an open-source project designed to provide a Python framework for working with seismological data. The key criterion for detecting foreshocks and aftershocks is the time difference between the arrival of the S-wave and P-wave (S-P interval). For events within approximately 13 km of the seismic station, those with an S-P interval of 3 to 3.5 seconds were specifically identified and separated. This approach enabled the collection of relevant events around the Kalanja station. Furthermore, single-station relocation methods are essential for accurately pinpointing the locations of events associated with the main earthquake located southwest of the Kalanja station (Havskov et al., 2012). After this detection, we used a set of commands to cut and edit aftershocks and foreshocks.

Anisotropy parameters were obtained by Anisomat+ software following the above steps, which included 303 results and 147 nulls. Anisotropy parameters were obtained by Anisomat+ software following the above steps, which included 303 results and 147 nulls. Figure 5 shows an example of the determination of anisotropy parameters related to an event on October 30, 2020, and a null example related to an event on July 16, 2021.

In order to investigate the variation of anisotropy, the changes in these two parameters were investigated over time, which can be seen in figure 6 and figure 7.

4.2 Ambient Noise Interferometry (ANI)

For processing seismic ambient noise data, we followed the workflow proposed by (Bensen et al., 2007; Lin et al., 2007) to obtain Rayleigh-wave noise correlation functions (NCFs). In the first step, the continuous vertical-component data were divided into one-hour segments (Movaghari & Javan, 2018; Movaghari et al., 2014). Then, we removed the mean, trend, and instrument response from these data. After the filtering data in the frequency range of 0.02-0.5 Hz, one-bit normalization and spectral whitening were applied to eliminate earthquakes and other instrumental irregularities. In the second step, the cross-correlations between one-hour segments were calculated and then linearly stacked

A)

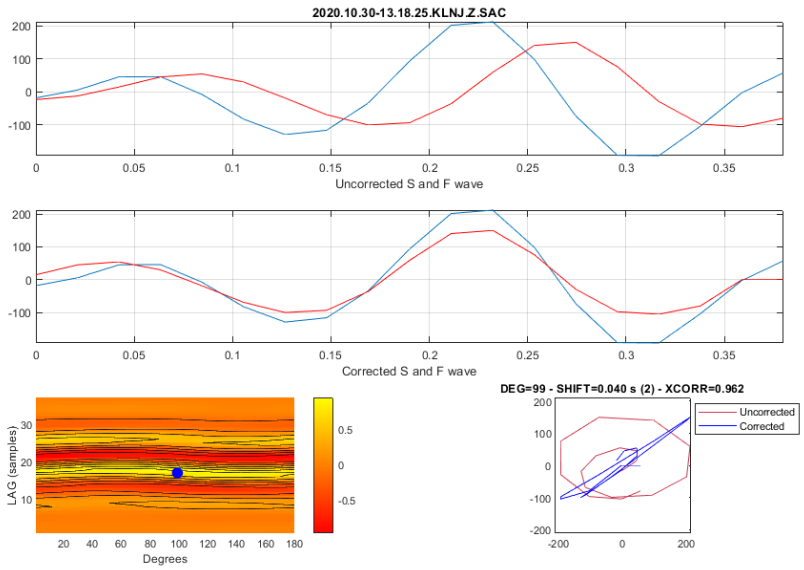

B)

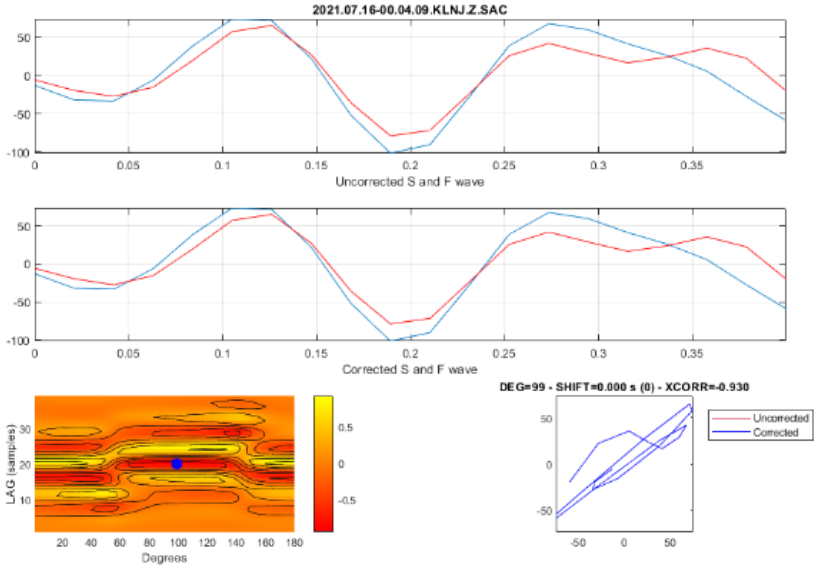

Figure 5. A) An example of the output of the anisomat+ code, where the (δt) and (ϕ) have been obtained. b) An example of a null output in which the S wave is not splitted and shows the linear particle motion.

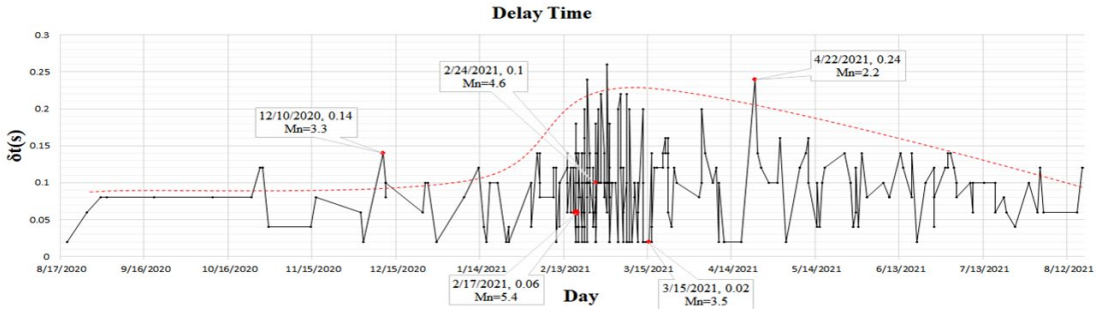

Figure 6. Show delay time parameter variation (δt). As can be seen, its value starts to increase one month before the earthquake and then starts to decrease with a gentle slope (the red dashed line shows the trend of parameter changes on average).

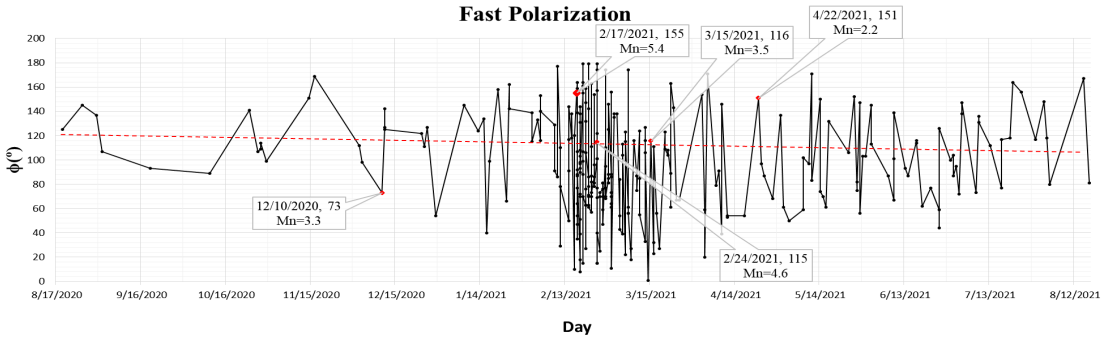

Figure 7. Display fast direction polarization parameter variation (ϕ). It is clear that before the earthquake, its values were fluctuated, and 6 months after the earthquake, the values have not reached a stable state (medium-sized red line is the value of the parameter in the entire period).

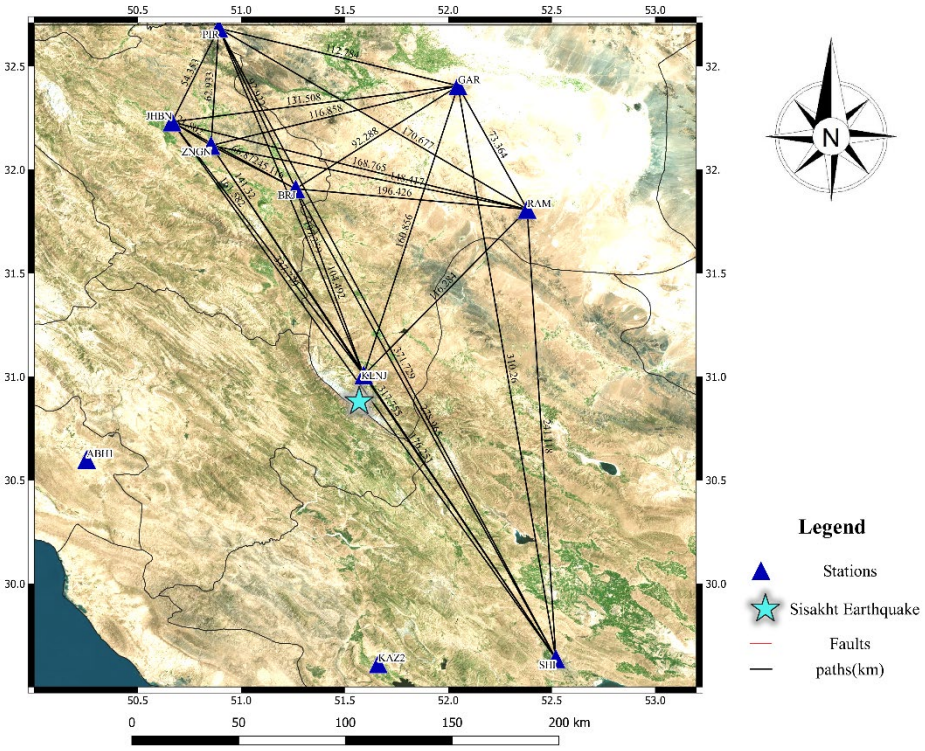

Figure 8. All inter-station paths to obtain the noise correlation functions.

to obtain the final NCF for each station pair. Figure 8 and Figure 9 show the inter-station paths and corresponding NCFs in this study.

We calculated the dispersion curves using the FTAN method (Levshin et al., 1972). This method is implemented in the computer programs in seismology (CPS) package (Herrmann, 2013) for the stacked NCFs.

The FTAN method involves selecting a time window centered around the first mode of the Rayleigh waveform for each NCF. The windowed data is then filtered using band-pass filters and the amplitude of each filtered trace is calculated using the analytical signal. A Gaussian filter is used to perform the filtering operation, with its center in the desired frequency range. The filtered traces are sorted by frequency and placed in a matrix, creating an energy diagram. The dominant dispersing curve is typically represented by the maximum range in

each column of the matrix. Noisy and invalid measurements can be visually removed at this stage. A suitable filter is applied to smooth the scattering curve and separate it from the rest of the signal. The final Rayleigh wave group velocity dispersion curves are depicted in Figure 10.

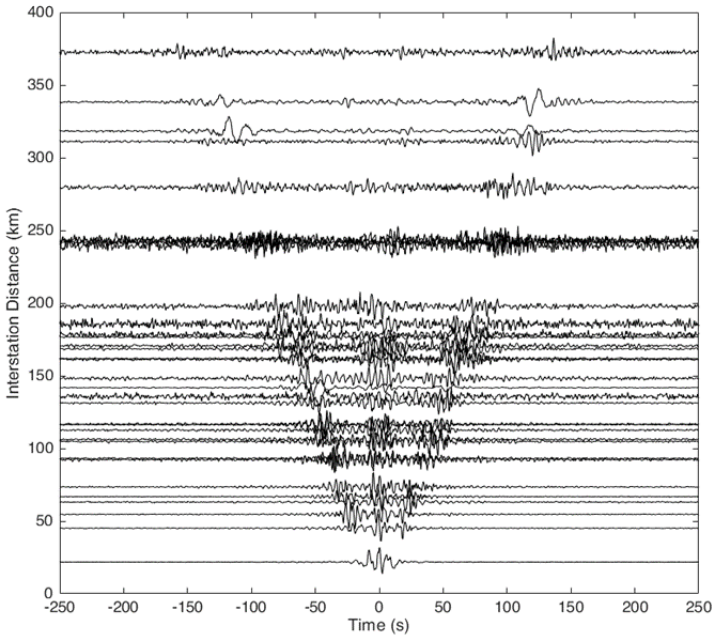

Figure 9. Noise Cross-correlation functions (NCF) for all station-pairs used in the region.

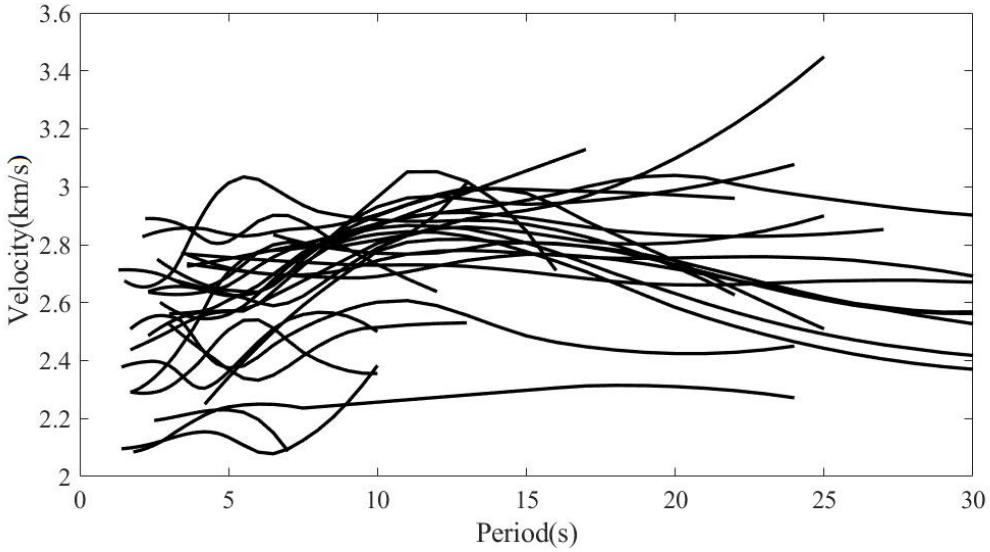

Figure 10. Rayleigh wave group velocity dispersion curves for all station pairs used in the study area.

According to (Smith & Dahlen, 1973), in an anisotropic medium and at a certain frequency ω, the group velocity variation can be written as follows:

$$U(\omega,\psi) = C_0 + a_1(\omega)\cos(2\phi) + a_2(\omega)\sin(2\phi) + a_3(\omega)\cos(4\phi) + a_4(\omega)\sin(4\phi)$$

In which C_0 is the isotropic term, ϕ is the

ray propagation azimuth and a1, a2, a3, and a4 are azimuthal anisotropic coefficients. The terms 2ϕ and 4ϕ denote a periodicity of 180° and 90°, respectively, and account for the azimuthal variations. The 4ϕ parts of this equation are negligible due to the small contribution group velocity variations (Montagner & Nataf, 1986).

Considering that the studied earthquake was located at a depth of 10 kilometers, we selected periods of 8, 10, and 12 s from the obtained group velocity dispersion curves due to these periods are sensitive to the depth range of 5 to 15 km. Figure 11 shows the azimuthal distribution of group velocities for each period. By fitting the whole raw dispersion data (red and blue dots) to an even-order harmonic (blue line), the anisotropic parameters are estimated.

The average direction of the fast axis for the periods of 8, 10, and 12 s before and after the earthquake are 156° and 150°, respectively. This value for processing all data is 152°. By comparing the obtained results, we conclude that there is no significant change in the direction of the fast axis before and after the earthquake. Considering that the obtained results represent the average of velocity changes beneath inter-station paths, and according to the removal of data from two stations due to the gaps (ABH1 and KAZ2), the obtained results can be attributed to the point with the most ray path density which is about 50 km far from the earthquake location.

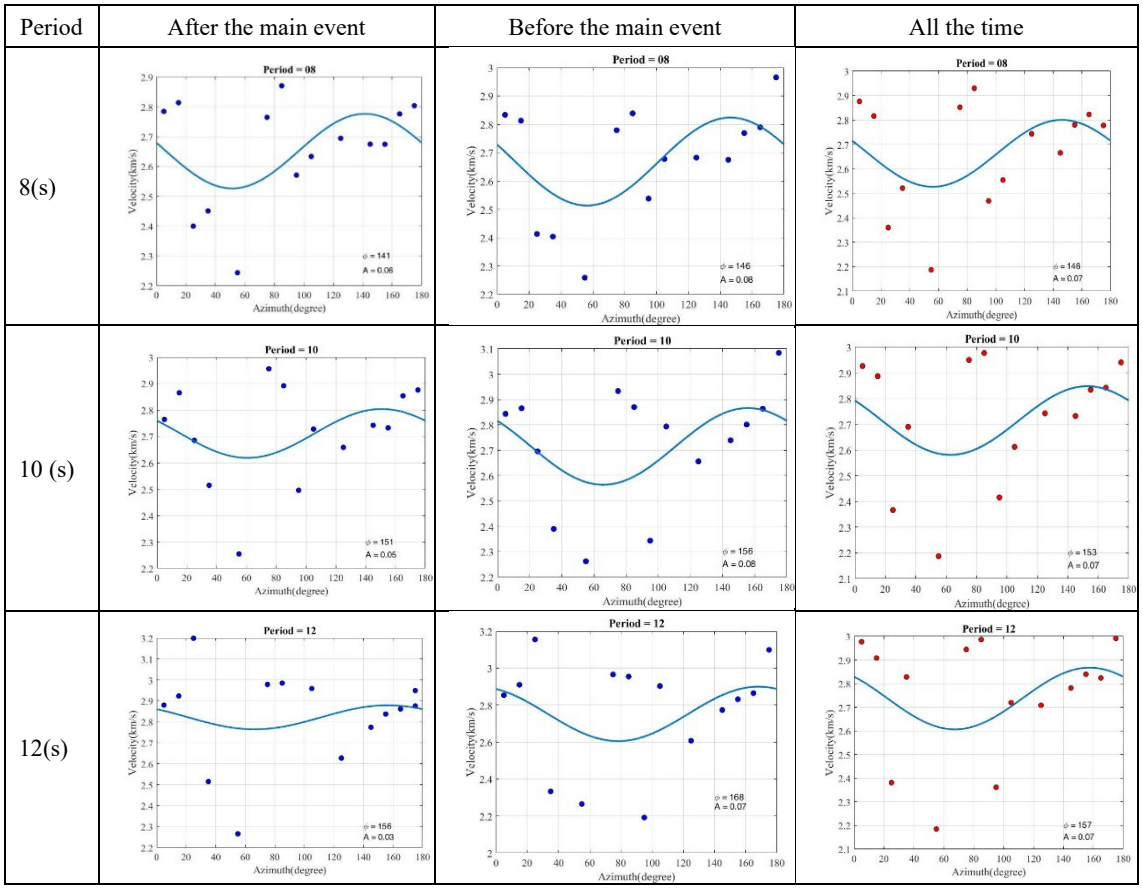

Figure 11. Azimuthal variation of Rayleigh-wave group velocities at periods of 8, 10, and 12 s obtained from inter-station paths.

5 Discussion and Conclusion

In this study we investigate the anisotropy before and after Sisakht's February 17, 2021 earthquake occurred in southwest of Iran using shear wave splitting (SWS) and ambient noise interferometry (ANI) methods. SWS is mainly sensitive to anisotropy in the upper mantle and lower crust, due to the path of the shear waves, but struggles with shallow crustal structures, potentially complicating post-earthquake anisotropy interpretation. In comparison, ANI is most sensitive to shallow crustal structures, which limits its ability to detect deeper anisotropy changes in the lower crust and upper mantle, potentially underrepresenting deep-seated changes after an earthquake. Combining these two method provides a complementary view of anisotropy changes before and after the earthquake.

In general, the anisotropy direction of the fast axis in the SWS method clearly illustrates the change in anisotropy direction following the earthquake. The results show that the average time delay (δt) before the earthquake is 0.08±0.01, and this value starts to increase from about one month before the earthquake and after the earthquake with an average of 0.1±0.01 (Figure 12). These changes can be due to various reasons such as the increase of cracks and fractures during the earthquake phases or fluid migration along pressure gradients between closely spaced microcracks and pores. Also, the estimation of the parameter (ϕ) shows significant increases and decreases in its values near the time of the earthquake. In this case, it appears that there was an increase in stress during the earthquake and an increase in cracks in various directions during the Sisakht earthquake.

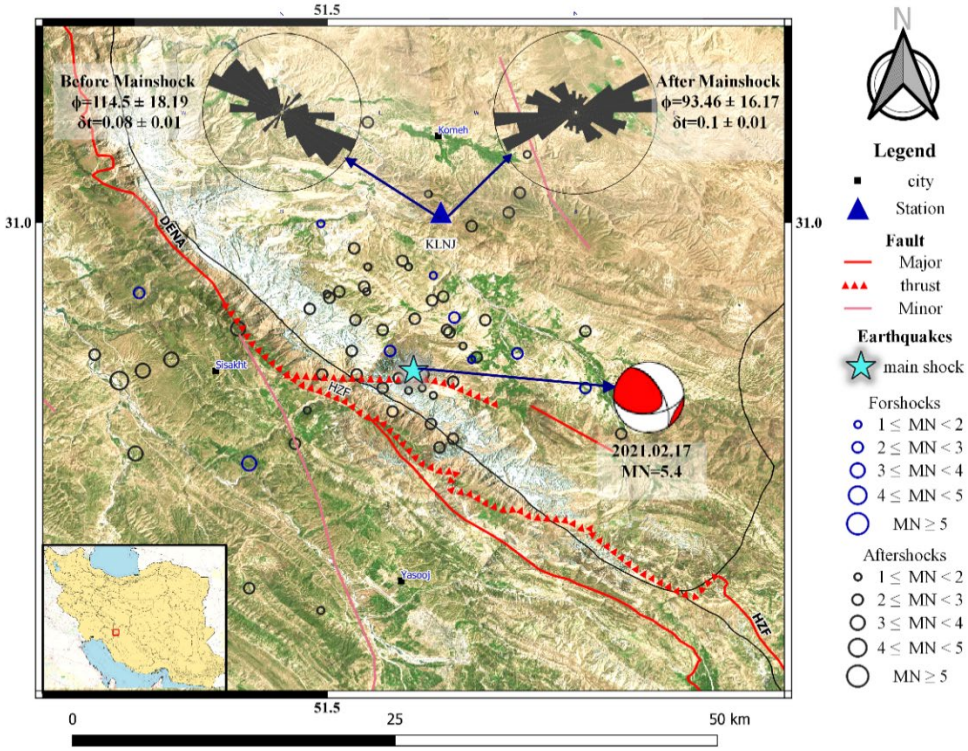

Figure 12. The tectonic map of the region including the epicenter of the main event and aftershocks and foreshocks and showing variation in the direction of anisotropy before and after the main earthquake. As can be seen in the figure, the direction of anisotropy after the earthquake is inclined from the northwest-southeast direction to the northeast-southwest direction.

Additionally, a comparison of the direction of anisotropy before the earthquake reveals an NW-SE trend, which is consistent with the High Zagros Fault (HZF), which is located 6 km from the epicenter of the Sisakht earthquake. However, after the earthquake, the anisotropy direction shows NE-SW anisotropy, which indicates that the main earthquake caused major cracks in this direction or the activation of a sub-fault in this direction.

In the ANI method, we processed continuous data from eight seismographic stations affiliated with the Iran Seismological Center (IRSC) to investigate azimuthal anisotropy in the study area. The need for continuous high-quality data can lead to the exclusion of certain stations, reducing spatial resolution and potentially introducing biases in unevenly distributed regions. In this case, the configuration of the station and data availability limited our study to the northeastern region of the earthquake (Figure 8). Three periods of 8, 10, and 12 seconds were used to calculate the amplitude and direction of the anisotropy. The sensitivity of these periods was estimated to be around the earthquake's depth (10 kilometers).

According to the obtained results, there is a slight change in the direction of anisotropy before and after the earthquake and a rotation of about 6° after the earthquake, which is not significant and can be within the estimations error. This was expected due to the lack of data and the removal of two stations, ABH1 and KAZ2. In general, the results of noise interferometry show that the direction of anisotropy in the studied area is in the northwest-southeast direction, which is in a good agreement with the geological

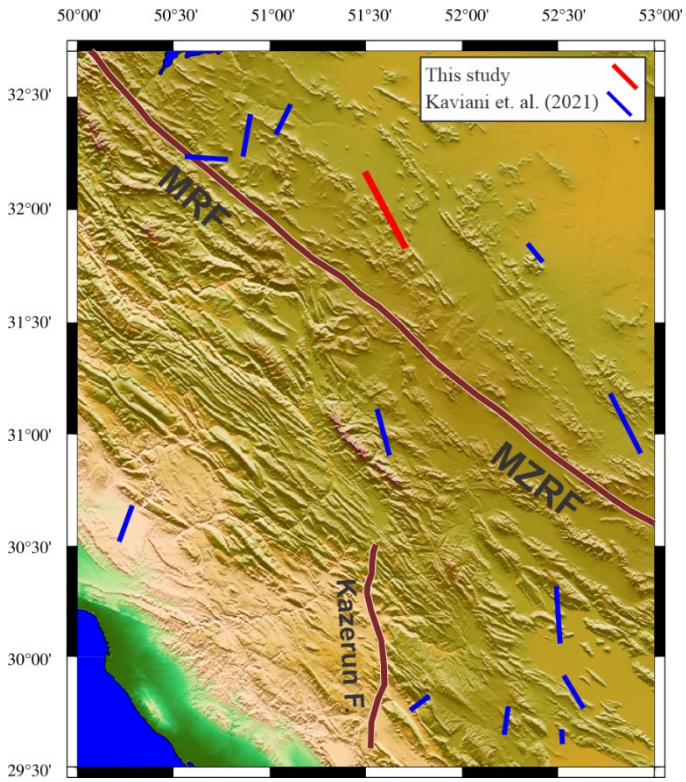

Figure 13. Comparison between the average result of our study from ANI (red bar) and the results of Kaviani et al. (2021) from the SWS method (blue bars).

structures of the area as well as the main fault of Dena, and consistent with the shear wave splitting results. The average direction of the fast axis is 152° which is subparallel to the result of Kaviani et al. (2021) from the SWS method in central Zagros (Figure 13). According to the sensitivity of 8, 10, and 12 s to the shallow depths, our result suggests a coherent deformation in central Zagros and SSZ in response to the compressional situation beneath the Iran plateau.

Acknowledgments

The authors would like to thank three anonymous reviewers for providing valuable comments and suggestions that improved the initial and revised versions of the manuscript. Some figures were made using the Open-Source Geospatial Foundation Project. http://qgis.org. We acknowledge the Iranian Seismological Center (IRSC) for providing the data used for this research.

References

Becker, T. W., Kustowski, B., & Ekström, G. (2008). Radial seismic anisotropy as a constraint for upper mantle rheology. *Earth and Planetary Science Letters*, *267*(1-2), 213-227.

Bensen, G., Ritzwoller, M., Barmin, M., Levshin, A. L., Lin, F., Moschetti, M., Shapiro, N., & Yang, Y. (2007). Processing seismic ambient noise data to obtain reliable broad-band surface wave dispersion measurements. *Geophysical journal international*, *169*(3), 1239-1260.

Boness, N. L., & Zoback, M. D. (2006). Mapping stress and structurally controlled crustal shear velocity anisotropy in California. *Geology*, *34*(10), 825-828.

Chao, K., & Peng, Z. (2009). Temporal changes of seismic velocity and anisotropy in the shallow crust induced by the 1999 October 22 M 6.4 Chia-Yi, Taiwan earthquake. *Geophysical Journal International*, *179*(3), 1800-1816.

Crampin, S. (1985). Evaluation of anisotropy by shear-wave splitting. *Geophysics*, *50*(1), 142-152.

Crampin, S., & Gao, Y. (2006). A review of techniques for measuring shear-wave splitting above small earthquakes. *Physics of the earth and planetary interiors*, *159*(1-2), 1-14.

Crampin, S., & Peacock, S. (2008). A review of the current understanding of seismic shear-wave splitting in the Earth's crust and common fallacies in interpretation. *Wave Motion*, *45*(6), 675-722.

Forsyth, D. W. (1975). The early structural evolution and anisotropy of the oceanic upper mantle. *Geophysical Journal International*, *43*(1), 103-162.

Hatzfeld, D., & Molnar, P. (2010). Comparisons of the kinematics and deep structures of the Zagros and Himalaya and of the Iranian and Tibetan plateaus and geodynamic implications. *Reviews of Geophysics*, *48*(2).

Havskov, J., Bormann, P., & Schweitzer, J. (2012). Seismic source location. In *New Manual of seismological observatory practice 2 (NMSOP-2)* (pp. 1-36). Deutsches GeoForschungsZentrum GFZ.

Herrmann, R. B. (2013). Computer programs in seismology: An evolving tool for instruction and research. *Seismological Research Letters*, *84*(6), 1081-1088.

Kaviani, A., Mahmoodabadi, M., Rümpker, G., Pilia, S., Tatar, M., Nilfouroushan, F., Yamini-Fard, F., Moradi, A., & Ali, M. Y. (2021).

Mantle-flow diversion beneath the Iranian plateau induced by Zagros' lithospheric keel. *Scientific reports*, *11*(1), 1-12.

Levshin, A. L., Pisarenko, V., & Pogrebinsky, G. (1972). On a frequency-time analysis of oscillations. Annales de geophysique,

Lin, F.-C., Ritzwoller, M. H., Townend, J., Bannister, S., & Savage, M. K. (2007). Ambient noise Rayleigh wave tomography of New Zealand. *Geophysical journal international*, *170*(2), 649-666.

Long, M. D., & Silver, P. G. (2009). Shear wave splitting and mantle anisotropy: Measurements, interpretations, and new directions. *Surveys in Geophysics*, *30*, 407-461.

Mahmoodabadi, M., Yaminifard, F., Tatar, M., & Kaviani, A. (2020). Shear wave velocity structure of the upper-mantle beneath the northern Zagros collision zone revealed by nonlinear teleseismic tomography and Bayesian Monte-Carlo joint inversion of surface wave dispersion and teleseismic P-wave coda. *Physics of the Earth and Planetary Interiors*, *300*, 106444.

Mirzaei, N., Mengtan, G., & Yuntai, C. (1998). Seismic source regionalization for seismic zoning of Iran: major seismotectonic provinces. *Journal of earthquake prediction research*, *7*, 465-495.

Montagner, J. P., & Nataf, H. C. (1986). A simple method for inverting the azimuthal anisotropy of surface waves. *Journal of Geophysical Research: Solid Earth*, *91*(B1), 511-520.

Motaghi, K., Shabanian, E., Tatar, M., Cuffaro, M., & Doglioni, C. (2017). The south Zagros suture zone in teleseismic images. *Tectonophysics*, *694*, 292-301.

Mousavi, S. H., Mirzaei, N., & Shabani, E. (2014). A declustered earthquake catalog for the Iranian Plateau. *Annals of geophysics*, *57*(6).

Mouthereau, F., Lacombe, O., & Vergés, J. (2012). Building the Zagros collisional orogen: timing, strain distribution and the dynamics of Arabia/Eurasia plate convergence. *Tectonophysics*, *532*, 27-60.

Movaghari, R., & Doloei, G. J. (2020). 3-D crustal structure of the Iran plateau using phase velocity ambient noise tomography. *Geophysical Journal International*, *220*(3), 1555-1568.

Movaghari, R., & Javan, D. G. (2018). Upper Crustal Structure of South West of Tehran Using Borehole Ambient Noise Tomography. *Journal of the Earth and Space Physics*, *44*(2). https://doi.org/10.22059/jesphys.2018.237090.1006914

Movaghari, R., Javan Doloei, G., Nowrozi, M., & Sadidkhouy, A. (2014). Velocity structure of south-east of Iran based on ambient noise analysis. *Journal of the Earth and Space Physics*, *40*(2), 17-30.

Movaghari, R., JavanDoloei, G., Yang, Y., Tatar, M., & Sadidkhouy, A. (2021). Crustal radial anisotropy of the Iran plateau inferred from ambient noise tomography. *Journal of Geophysical Research: Solid Earth*, *126*(4), e2020JB020236.

Nicolson, H., Curtis, A., Baptie, B., & Galetti, E. (2012). Seismic interferometry and ambient noise tomography in the British Isles. *Proceedings of the Geologists' Association*, *123*(1), 74-86.

Pastori, M., Valoroso, L., Piccinini, D., Wustefield, A., Zaccarelli, L., Bianco, F., Kendall, M., Di Stefano,

R., Chiaraluce, L., & Di Bucci, D. (2012). Crustal fracturing and presence of fluid as revealed by seismic anisotropy: case histories from seismogenic areas in the Apennines (Italy). *Bollettino di Geofisica Teorica ed Applicata*.

Paul, A., Hatzfeld, D., Kaviani, A., Tatar, M., & Péquegnat, C. (2010). Seismic imaging of the lithospheric structure of the Zagros mountain belt (Iran). *Geological Society, London, Special Publications*, *330*(1), 5-18.

Piccinini, D., Pastori, M., & Margheriti, L. (2013). ANISOMAT+: An automatic tool to retrieve seismic anisotropy from local earthquakes. *Computers & geosciences*, *56*, 62-68.

Roux, P., Sabra, K. G., Kuperman, W. A., & Roux, A. (2005). Ambient noise cross correlation in free space: Theoretical approach. *The Journal of the Acoustical Society of America*, *117*(1), 79-84.

Sadeghi-Bagherabadi, A., Margheriti, L., Aoudia, A., & Sobouti, F. (2018). Seismic anisotropy and its geodynamic implications in Iran, the easternmost part of the Tethyan Belt. *Tectonics*, *37*(12), 4377-4395.

Shapiro, N. M., & Campillo, M. (2004). Emergence of broadband Rayleigh waves from correlations of the ambient seismic noise. *Geophysical Research Letters*, *31*(7).

Smith, M. L., & Dahlen, F. (1973). The azimuthal dependence of Love and Rayleigh wave propagation in a slightly anisotropic medium. *Journal of Geophysical Research*, *78*(17), 3321-3333.

Vecsey, L., Plomerová, J., & Babuška, V. (2008). Shear-wave splitting measurements—Problems and solutions. *Tectonophysics*, *462*(1-4), 178-196.

Zarunizadeh, Z., Motaghi, K., Movaghari, R., Yang, Y., & Priestley, K. (2024). Seismological constraints on the lithosphere-asthenosphere system beneath the central and east Iranian Plateau. *Tectonophysics*, 230215.